remote sensing

MDPI

Supplementary Materials

Simultaneous Remote Sensing of $HD^{16}O/H_2{}^{16}O$ Profile Using Differential Absorption Lidar: A Feasibility Analysis

Saifen Yu [1,2], Zhen Zhang [1,2,*] and Haiyun Xia [1,2,3]

[1] State Key Laboratory of Climate System Prediction and Risk Management, Nanjing University of Information Science and Technology, Nanjing 210044, China; sfyu@nuist.edu.cn (S.Y.); hsia@ustc.edu.cn (H.X.)
[2] School of Atmospheric Physics, Nanjing University of Information Science and Technology, Nanjing 210044, China
[3] School of Earth and Space Science, University of Science and Technology of China, Hefei 230026, China
* Correspondence: zhenzhang@nuist.edu.cn

1 Supplementary Materials

1.1 Selection of system parameters

In this study, most system parameters such as pulse repetition frequency, telescope aperture, field of view, optical transmission efficiency of the transmitter and receiver, the dark count rate and noise-equivalent power of the superconducting detector, and the sampling rate of the multi-channel scaler are adopted from our previous lidar system [1]. Some parameters are specifically adjusted for the simultaneous detection of $H_2{}^{16}O$ and $HD^{16}O$. The scanning wavelength range and reference wavelength are chosen according to the absorption features of $H_2{}^{16}O$ and $HD^{16}O$. Since the detection wavelength in this work is near 1554 nm, where fiber laser components are more mature and efficient, the simulated pulse energy is set to 300 μJ, compared with 40 μJ in the previous system operating around 1572 nm. In addition, the quantum detection efficiency of the superconducting detector is improved from 31.5% to 51% at 1554 nm, enhancing overall measurement performance.

1.2 Atmospheric molecular extinction mode and aerosol particle extinction mode

For the general case, the simulation adopts the 532 nm atmospheric molecule extinction mode and aerosol particle extinction mode. The backscattered coefficient β_m (km^{-1}/sr) and extinction coefficient α_m (km^{-1}) of atmospheric molecules are expressed by height Z as

$$\beta_m(Z) = 1.54\times10^{-3}\exp(-Z/7) \tag{S1}$$

$$\alpha_m(Z) = \beta_m(Z)\times 8\pi/3 \tag{S2}$$

The backscattered coefficient β_a (km^{-1}/sr) and extinction coefficient α_a (km^{-1}) of atmospheric aerosols are expressed by height Z as

$$\beta_a(Z) = 2.47\times10^{-3}\exp(-Z/2) + 5.13\times10^{-6}\exp\left[-(Z-20)^2/36\right] \tag{S3}$$

$$\alpha_a(Z) = \beta_a(Z)\times 50 \tag{S4}$$

The relationship between the backscattered coefficients of atmospheric molecules and aerosols and the optical wavelength can be expressed as

 https://doi.org/10.3390/rs18020212

$$\frac{\beta_a(\lambda_1, Z)}{\beta_a(\lambda_2, Z)} = \left(\frac{\lambda_1}{\lambda_2}\right)^{-1} \quad \text{(S5)}$$

$$\frac{\beta_m(\lambda_1, Z)}{\beta_m(\lambda_2, Z)} = \left(\frac{\lambda_1}{\lambda_2}\right)^{-4} \quad \text{(S6)}$$

where λ_1 and λ_2 represent different wavelengths of 532 nm and 1554 nm, respectively. Based on the above equations, the atmospheric backscattering and extinction coefficients corresponding to the investigated wavelengths of $H_2{}^{16}O$ and $HD^{16}O$ can be obtained.

For the case with pollution, the simulation adopts the atmospheric aerosol particle extinction mode with highest decile described in [2]. The extinction-to-backscatter ratio α_a/β_a (lidar ratio) is set to 40 sr. For the case of severe pollution or extreme weather conditions, the lidar performance is primarily affected by variations in the backscattered and extinction coefficients. To account for this, the extinction coefficient near the ground (α_{a0}) is set to 10 km^{-1} and the extinction coefficient profile at higher altitudes is modeled using a Gaussian profile [2], in order to estimate the potential random errors.

1.3 Atmospheric temperature, pressure and $H_2{}^{16}O$ modes

The absorption coefficients spectra of $H_2{}^{16}O$ and $HD^{16}O$ depend on atmospheric conditions. Commonly used atmospheric models include Tropical, Mid-Latitude Summer (MLS), Mid-Latitude Winter (MLW), Sub-Arctic Summer (SAS), Sub-Arctic Winter (SAW), and the 1976 U.S. Standard Atmosphere. Each model describes distinct vertical profiles of temperature, pressure, air density, $H_2{}^{16}O$, and other gas constituents. Among these, the MLS, MLW, and the 1976 U.S. Standard Atmosphere models generally represent the atmospheric profiles characteristics of mid-latitude regions. Figure S1 shows the temperature, pressure and $H_2{}^{16}O$ profiles within 2 km altitude, with the primary differences arising from the distributions of temperature and $H_2{}^{16}O$. Figure S2 shows that when the uncertainties in temperature, pressure, and frequency are set to −1 K, −1 hPa, and −0.5 MHz, respectively, the resulting systematic errors are equal in magnitude but opposite in sign to those obtained for positive uncertainties.

1.4 Lidar performance under different atmospheric conditions (clean, polluted, extreme polluted)

To assess the lidar retrieval performance under different aerosol load conditions, relative random errors are calculated for both clean and polluted atmospheric conditions using the aerosol backscattered and extinction coefficient models presented in Section 1.2. The results are shown in Figure S3. Although aerosol extinction in polluted conditions attenuates the lidar signal and weakens the return from distant ranges, the signal enhancement within the near-surface to boundary-layer region is much more significant. The enhanced backscatter is sufficient to compensate for the attenuation, ensuring high-quality signals within the target observation range. As a result, the corresponding random errors in this case are smaller than those under clean atmospheric conditions. Furthermore, Figure S4 shows the extreme case of severe pollution, where the lidar signal rapidly attenuates with altitude, leading to a rapid increase in random errors at heights near 1 km. In this scenario, the lidar detection range is limited with a primary focus on measuring $H_2{}^{16}O$ and $HD^{16}O$ at near-ground altitudes.

In addition, during the simulation of lidar backscatter signals, the $H_2{}^{16}O$ content is the dominant factor influencing the signal-to-noise ratio (SNR) and random errors by affecting the absorption strength. Figure S5 compares the retrieved SNR and random errors under the three atmospheric models. As expected, the random errors for the 1976 U.S. Standard atmosphere lie between those of the MLS and MLW models, and all three

models exhibit similar error variation patterns with wavelength and altitude. Under the selected absorption lines and system parameters for $H_2^{16}O$ and $HD^{16}O$ simulations, higher $H_2^{16}O$ concentrations result in smaller retrieval errors.

1.5 Mixing ratio errors of $H_2^{16}O$, $HD^{16}O$ and δD

The standard error of the retrieved mixing ratios is determined by the standard error of the fitted areas, which inherently accounts for both random and systematic errors through the spectral fitting process. The fitting errors of the integrated area are typically calculated using the least-squares method, based on data residuals and the model's sensitivity through the parameter covariance matrix. In general, larger fitting residuals result in greater errors in the fitted areas, leading to increased standard error in the retrieved mixing ratios. The standard error of δD is then determined based on the principle of error propagation, which accounts for the uncertainties in both $H_2^{16}O$ and $HD^{16}O$, which is expressed as

$$\sigma_{\delta_D} = \frac{1000}{R_{\mathrm{SMOW}}} \sqrt{\left(\frac{\sigma_{HD^{16}O}}{H_2^{16}O}\right)^2 + \left(\frac{HD^{16}O \cdot \sigma_{H_2^{16}O}}{\left(H_2^{16}O\right)^2}\right)^2} \tag{S7}$$

where RSMOW is defined as 3.1152×10^{-4} according to Standard Mean Ocean Water. $\sigma_{HD^{16}O}$ and $\sigma_{H_2^{16}O}$ are the standard error of $HD^{16}O$ and $H_2^{16}O$, respectively.

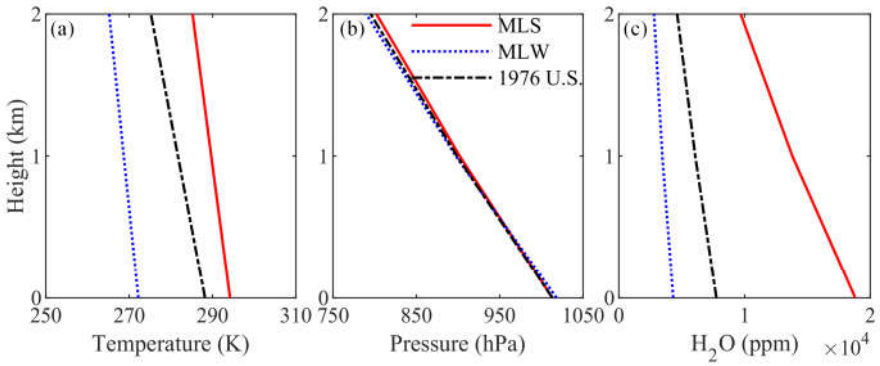


Figure S1. Atmospheric (a) temperature, (b) pressure, and (c) $H_2^{16}O$ profiles of different atmospheric models within 2 km altitude.

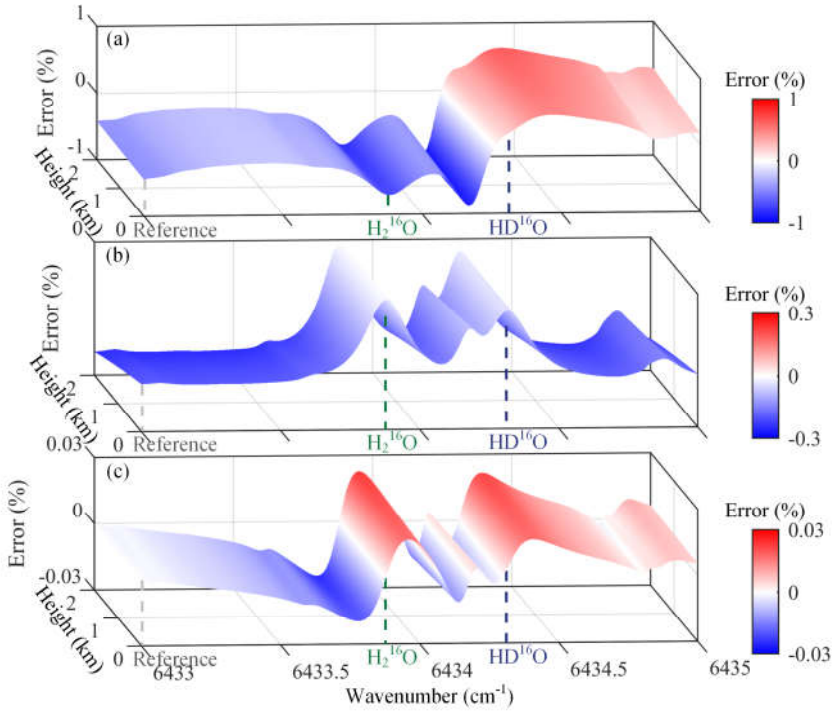


Figure S2. The relative systematic errors for gas mixing ratio profiles retrieval with (a) temperature uncertainty of -1 K, (b) pressure uncertainty of -1 hPa, (c) frequency uncertainty of -0.5 MHz.

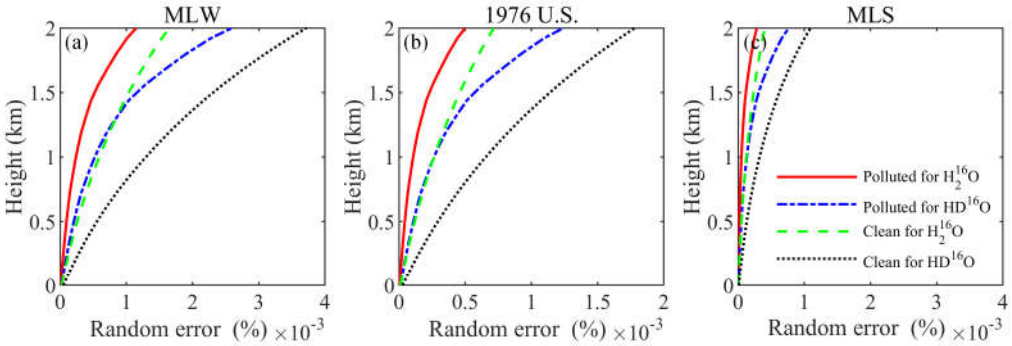


Figure S3. Relative random errors of $H_2^{16}O$ and $HD^{16}O$ in clean and polluted atmospheres. (a) MLW model, (b) 1976 U.S. Standard atmosphere and (c) MLS model.

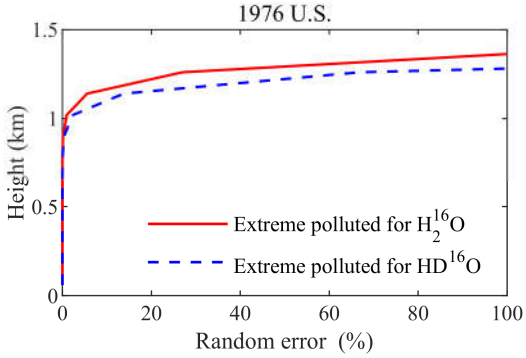


Figure S4. Relative random errors of $H_2^{16}O$ and $HD^{16}O$ corresponding to the 1976 U.S. Standard atmosphere under severe pollution (with a near-ground extinction coefficient of 10 km^{-1}).

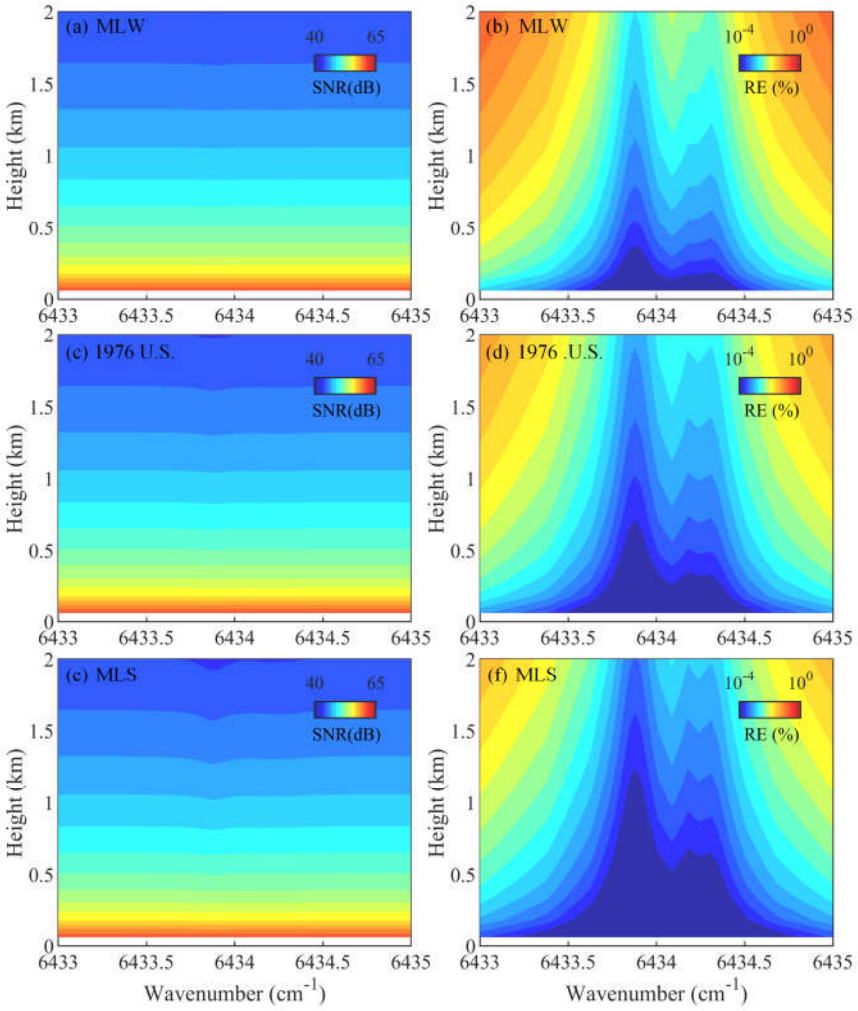


Figure S5. SNR and random error of the simulated DIAL backscattered signals under the MLW model (a–b), the 1976 U.S. Standard atmosphere (c–d) and the MLS model (e–f).

References

1. Yu, S.; Zhang, Z.; Li, M; Xia, H. Multi-frequency differential absorption lidar incorporating a comb-referenced scanning laser for gas spectrum analysis. *Opt. Express*, **2021**, 29, 12984–12995.
2. Hamperl, J.; Capitaine, C.; Dherbecourt, J.B.; Raybaut, M.; Chazette, P.; Totems, J.; Grouiez, B.; Régalia, L.; Santagata, R.; Evesque, C.; Melkonian, J.M. Differential absorption lidar for water vapor isotopologues in the 1.98 μm spectral region: sensitivity analysis with respect to regional atmospheric variability, *Atmos. Meas. Tech.* **2021**, 14, 6675–6693.

Disclaimer/Publisher's Note: The statements, opinions and data contained in all publications are solely those of the individual author(s) and contributor(s) and not of MDPI and/or the editor(s). MDPI and/or the editor(s) disclaim responsibility for any injury to people or property resulting from any ideas, methods, instructions or products referred to in the content.